VOLUME 4, NUMBER 11, NOVEMBER 2004

NANO LETTERS

Rapid Prototyping of Site-Specific Nanocontacts by Electron and Ion Beam Assisted Direct-Write Nanolithography

Vidyut Gopal*,† and Velimir R. Radmilovic

National Center for Electron Microscopy, Lawrence Berkeley National Laboratory, Berkeley, California 94720

Chiara Daraio and Sungho Jin

Materials Science and Engineering Program, University of California, San Diego, La Jolla, California 92093

Peidong Yang

Department of Chemistry, University of California, Berkeley, California 94720

Eric A. Stach‡

National Center for Electron Microscopy, Lawrence Berkeley National Laboratory, Berkeley, California 94720

Received May 25, 2004; Revised Manuscript Received September 6, 2004

ABSTRACT

Rapid prototyping of bottom-up nanostructure circuits is demonstrated, utilizing metal deposition and patterning methodology based on combined focused ion and electron beam induced decomposition of a metal–organic precursor gas. Ohmic contacts were fabricated using electron beam deposition, followed by the faster process of ion beam deposition for interconnect formation. Two applications of this method are demonstrated: three-terminal transport measurements of Y-junction carbon nanotubes and fabrication of nanocircuits for determination of electromechanical degradation of silver nanowires.

Chemically synthesized one-dimensional (1D) nanostructures, including nanowires and nanotubes of various compositions, are the focus of intense research in nanoscience and technology.[1] Electrical transport in these 1D nanostructures forms the basis for many of their potential applications in electronics, photonics, and sensors. The development of techniques for rapid and accurate electrical testing would be an enabler for a wide variety of nanotechnology research.

* Corresponding author: E-mail: vidyut.gopal@spansion.com.
† Present address: Spansion LLC, Sunnyvale, CA 94088.
‡ Present address: School of Materials Engineering, Purdue University, West Lafayette, IN 47906.

10.1021/nl0492133 CCC: $27.50
Published on Web 10/15/2004

Traditionally, electron beam lithography (EBL) in a scanning electron microscope (SEM) is used to fabricate prototypical nanocircuits for electrical characterization. Metal deposition and patterning by EBL constitutes a time-consuming multistep process often resulting in poor yield. It is difficult to locate individual nanostructures underneath a thick polymethyl-methacrylate (PMMA) resist layer in a SEM. This leads to frequent misalignment of patterns. Incomplete or improper lift-off is also a frequent cause of poor yield.

Direct-write nanopatterning by electron and ion beam induced deposition has the potential to avoid the process complexity of EBL in nanocircuit fabrication.[2,3] A metal−organic precursor is heated and the vaporized species is injected into the path of a scanning electron or ion beam. The adsorbed gas molecules are decomposed upon exposure to the beam, which results in the localized deposition of a metal-rich conductive material. The process can be described as electron or ion beam assisted localized chemical vapor deposition (CVD).[4−6] This is a well-established process, and researchers have successfully deposited a variety of metals, including Pt, Au, W, and Al, using this technique.[4] In this article, we report new and unique applications of this technique for the fabrication of contacts and interconnects in prototypical circuits incorporating 1D nanostructures. By controlling the raster time and dimensions, the metal can be deposited and patterned into desirable shapes and sizes in a single step. Combined with in-situ SEM imaging, 1D nanostructures of interest can be rapidly located and interconnected to larger electrodes in a few minutes. One potential drawback to this approach is the considerable delocalization or spread of metallic species outside of the electron or ion beam raster area. We have extensively characterized the spread of Pt, both by the surface sensitive technique of time-of-flight secondary ion mass spectrometry (TOF−SIMS) and by measuring the leakage current between closely spaced pairs of metallic lines. The results of this investigation are reported in a separate publication and are only briefly discussed here.[7] TOF−SIMS surface ion maps detected a spread of Pt ions several micrometers beyond the beam raster area, providing evidence for widespread surface decoration. We proposed that enhanced surface mobility of the decomposed species due to beam-induced heating is responsible for the spread.[7] According to Melngailis, simulations indicate that there are severe thermal spikes microscopically in the vicinity of an incident ion.[4] As the incident ion traverses the substrate, the atoms in the immediate vicinity of the ion's path are so severely disturbed as to reach temperatures of several thousand degrees. Though the thermal spikes relax in less than one nanosecond, they may play an important role in many phenomena, including sputtering and surface diffusion, which could cause adsorbed atoms to spread far from the area of incidence of the primary beam. The spread results in the decoration of the nanostructure of interest with metallic species and provides a leakage pathway during biasing. A method for overcoming the delocalization problem by the combination of electron beam deposition with ion beam deposition is reported here. Two unique applications that were enabled by this technique are discussed. The first is three-terminal transport measurements of Y-junction carbon nanotubes. The second is fabrication of contacts and interconnects to metallic nanowires on very thin (100 nm) electron transparent membranes for in-situ transmission electron microscopy (TEM) imaging of electromechanical degradation.

An FEI Strata 235 M dual beam (FIB/SEM) system was used for deposition. A metal−organic precursor, trimethyl-cyclopentadienyl-platinum ($(CH_3)_3CH_3C_5H_4Pt$), was heated to 40 °C. The vaporized species was injected by means of a 0.7 mm diameter needle into the path of the scanning beam. Both electron and ion beam depositions were performed at normal beam incidence, with the sample stage being tilted by 52° in order to perform the latter deposition (the angle of inclination between the FIB and SEM columns). The stage was maintained at room temperature and the chamber pressure was about 10^{-5} Torr during the deposition. Electron beam deposition was carried out at primary beam energy of 10 keV, beam current of 2 nA, and nominal beam diameter of 7 nm. Ion beam deposition was carried out with Ga^+ ions at an energy of 30 keV and beam current of 30 pA. The pixel dwell time was 0.4 μs, with no overlap between pixels. The diameter (spot size) of the ion beam is not accurately known. Pt lines connecting photolithographically prepatterned Au electrodes on oxidized Si substrates were deposited to test the conductivity.[7] The beam raster dimensions were fixed to be 40 μm in length and 250 nm in width. The resistivity of electron beam and ion beam deposited Pt are compared in Figure 1a. It is noteworthy that the time employed for ion beam deposition was 10 times less than that for electron beam deposition, i.e., ion beam deposition is both faster and results in more conductive material than electron beam deposition. The rapid drop of resistivity with low-temperature annealing and the subsequent saturation at higher temperatures is indicative of point defect activity such as vacancy annealing, rather than phase transformations in this material. To investigate temperature stability, a sample consisting of both electron and ion beam deposited Pt was heated in-situ in a TEM. Bright field images are shown in Figure 1a at room temperature and at 600 °C. Both types of deposition result in nanocrystalline Pt grains embedded in an amorphous carbon matrix. The ion beam deposited material has a darker contrast, indicative of higher Pt content than the electron beam material, which explains the higher conductivity of the former. There was no apparent phase transformation during the in-situ heating experiment, and the structure remained stable until 900 °C, when a Pt carbide phase was observed to precipitate. Thus, both ion and electron beam deposited Pt display very good high-temperature stability, an essential requirement for nanocontact applications.

Metal delocalization induced current leakage was characterized by depositing pairs of closely spaced Pt lines.[7] A comparison of the leakage resistance, plotted as a function of gap spacing, between electron and ion beam deposited Pt is shown in Figure 1b. The electron beam deposited material displayed leakage that increased exponentially as the gap spacing was reduced. In contrast, the leakage current due to

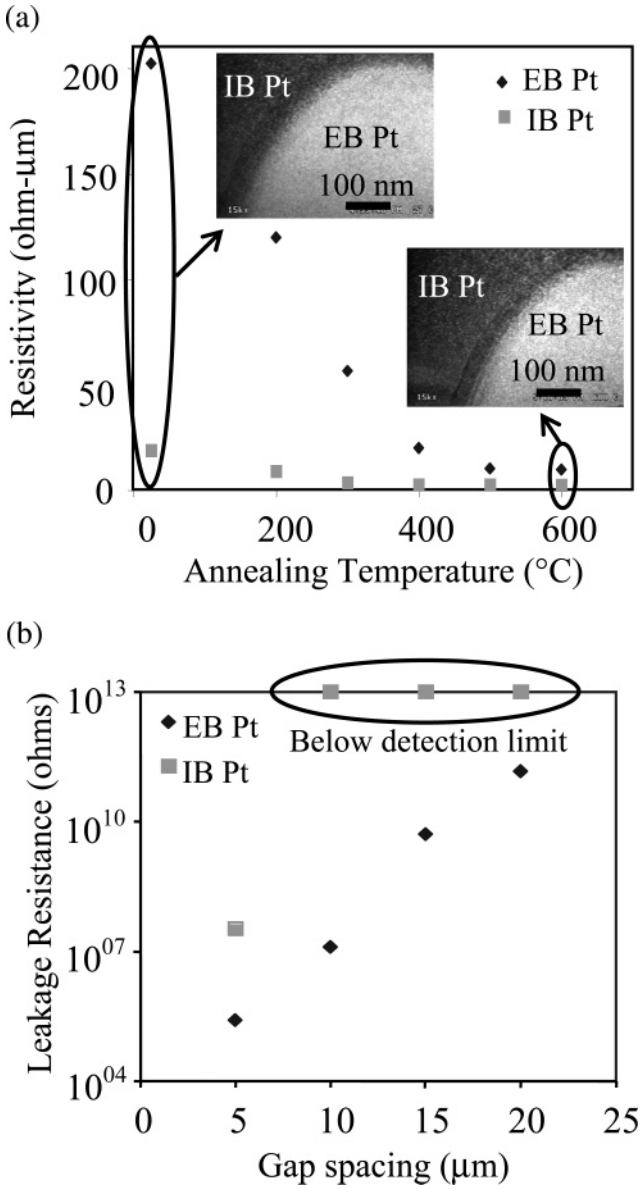

Figure 1. (a) Variation of the resistivity of electron and ion beam deposited Pt as a function of post-deposition annealing temperature. The rapid thermal annealing was carried out in an inert (N_2) atmosphere. (Inset): Cross-section TEM images of the microstructure of electron and ion beam deposited Pt at room temperature and 600 °C. (b) Comparison of the metallic spread-induced leakage resistance resulting from electron beam and ion beam deposition of Pt.

ion beam deposition was too low to be measured by our probe station (i.e., < 1 pA) for gap spacing that exceeded 5 μm. These data indicate that ion beam deposition should be chosen over electron beam deposition to fabricate nanocircuits, due to both superior conductivity and leakage characteristics. However, the ion beam deposition of Pt cannot be used to make contacts to the 1D nanostructures since exposure to the massive Ga ion beam would destroy the nanostructures of interest. Hence, a two-step process was adopted. Electron beam deposited Pt was used to make contacts to the nanostructures, taking care to minimize the time of deposition (<30 s) in order to prevent formation of a leakage pathway. The contacted nanostructures were

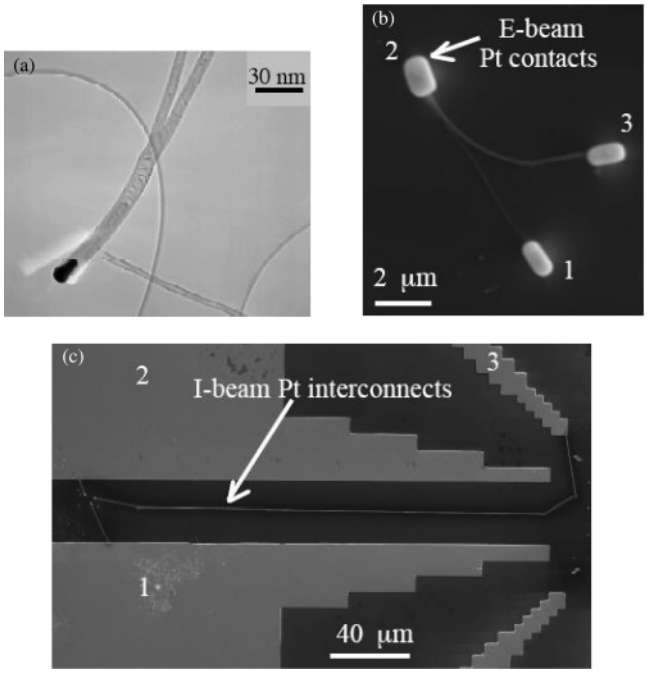

Figure 2. (a) Bright field TEM image of a Y-junction carbon nanotube. (b) SEM image of a Y-junction nanotube with contacts to the three terminals fabricated by electron beam assisted deposition of Pt. (c) SEM image of the same Y-junction nanotube after it had been interconnected to macroscale electrodes using ion beam Pt deposition.

subsequently interconnected to prepatterned electrodes using ion beam deposition, taking care not to expose the nanostructure to the ion beam. The utility of this approach is illustrated with the two examples.

Y-junction carbon nanotubes are three-terminal nanostructures where the branching of the nanotube is achieved during CVD synthesis by the introduction of Ti catalyst particles.[8] A bright field TEM image of a typical Y-junction nanotube is shown in Figure 2a. Owing to their unique structure, Y-junction nanotubes have the promise to act as miniaturized transistors with a potential applied to one terminal (gate) regulating the current between the other two terminals (source-drain).[9] Contacts were fabricated to the three terminals of a Y-junction nanotube using electron beam deposited Pt, as shown in Figure 2b. The nanotube was then interconnected to macroscale electrodes by ion beam Pt, without exposing it to the ion beam (Figure 2c). The results of two- and three-terminal transport measurements performed on the nanotube are shown in Figures 3a and 3b. The nanotube shown in Figure 2b was asymmetrical, i.e., the two branches had different diameters, and hence, different resistances, as confirmed by the two terminal electrical data (Figure 3a). The fact that the resistance between terminals 2−3 was nearly three orders of magnitude smaller than between terminals 1−2 also implied that the current measured was not due to Pt spread induced leakage. We confirmed this by depositing an identical contact geometry at a separate location without any nanotubes. The leakage currents were found to be below the detection limit (1 pA) of the measurement apparatus (Keithley 236 source measure unit (SMU)). The three terminal transport data (Figure 3b) show that a gate voltage

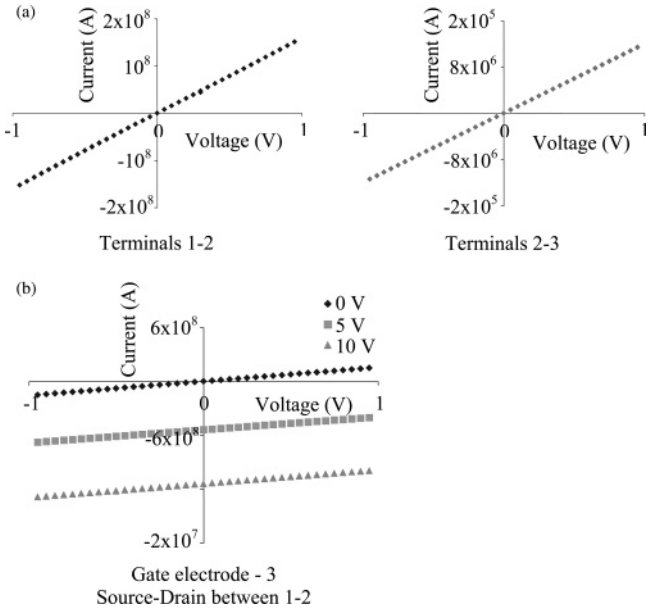

Figure 3. (a) Current−voltage data from two-terminal transport measurements of Y-junction nanotube. Note that the branch connecting terminals 2−3 is three orders of magnitude more conductive than the branch connecting terminals 1−2. (b) Current−voltage data from three-terminal transport measurements of a Y-junction nanotube. A gate voltage applied at terminal 3 regulates the source-drain current between terminals 1 and 2.

could indeed be used to regulate the channel current, as predicted by Papodopoulos et al.[10] A gate voltage applied to terminal 3 resulted in the translation of the linear $I-V$ characteristic between terminals 1 and 2, without change of slope. This is a manifestation of Kirchhoff's law of nodes at the nanoscale. Rectifying behavior was not observed, and the nanotube was determined to be metallic. Similar $I-V$ characteristics were obtained from several other Y-junction nanotubes from the same batch; each of them was metallic in nature. Thus, we have been successful in fabricating three very closely spaced contacts to Y-junction nanotubes in a rapid and reproducible manner, with none of the misalignment problems that might have resulted from the use of a traditional EBL process.

Electromechanical degradation of current carrying elements is of considerable interest due to the aggressive scaling of the feature sizes of interconnects. A novel approach was adopted to study current-induced degradation in metallic nanowires, namely, real-time TEM imaging during in-situ biasing. A specimen holder with four Be−Cu probes (Figure 4a) was fabricated for a JEOL 3010 TEM. The probes were connected to a Keithley 236 SMU for electrical measurements. Ag nanowires, synthesized in solution phase,[11] were dispersed on 100 nm thick Si_3N_4 electron transparent membranes, with prepatterned Au electrodes sputtered through a shadow mask (inset of Figure 4a). The membranes were prepared by depositing Si_3N_4 on Si, followed by backside chemical etching to open a 0.5 mm square window. The Ag nanowires were interconnected to the macroscale electrodes using the two-step electron beam/ion beam Pt deposition process (Figure 4b). The thin membrane would be destroyed in a conventional EBL process, especially

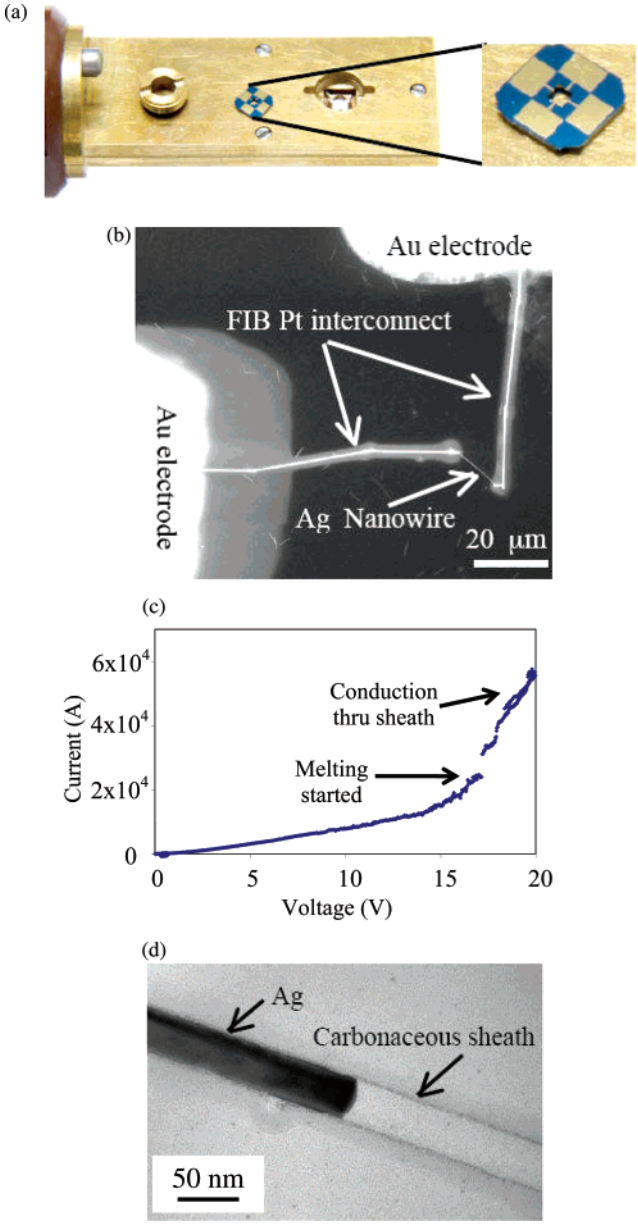

Figure 4. (a) Picture of the front piece of a TEM specimen holder with 4 Be−Cu probes for the in-situ biasing of one-dimensional nanostructures. (Inset): Si_3N_4 membrane specimen with prepatterned Au electrodes. (b) SEM image of Ag nanowire on a Si_3N_4 membrane interconnected to Au electrodes using electron beam and ion beam assisted Pt deposition. (c) Current−voltage data collected while simultaneously observing the Ag nanowire in a TEM. (d) Ag nanowire partially melted due to resistive heating. A carbonaceous sheath surrounding the nanowire continues to conduct current after the Ag core has melted.

during the resist spin coating step. Hence, direct writing in the dual beam FIB was an ideal specimen preparation method for this application. The nanowires were found to degrade chiefly by resistive heat induced melting. The $I-V$ characteristic of a typical Ag nanowire sample is shown in Figure 4c. The voltage was ramped up in increments of 50 mV every 10 s, while simultaneously imaging (in bright field) and videotaping the nanowire. As the voltage was ramped up, the slope of the $I-V$ curve became steeper, implying an apparent increase in conductivity. This was an artifact caused

due to the high contact resistance of the deposited Pt. The resistive heating helped to anneal the contacts, thus reducing the contact resistance. With continued bias ramping, the Ag nanowire began to melt. It was observed that the nanowire consisted of a core−sheath structure, and as the Ag core melted, a carbonaceous sheath was left behind. We believe that the melted Ag was partially incorporated into the sheath, because the nanowire continued to conduct current even after the core Ag had melted. Eventually, the core became discontinuous and the current was conducted by the sheath alone. At this stage the melting of the Ag core ceased and a partially melted nanowire remained.

In conclusion, we have developed a FIB based direct-write technique for the rapid fabrication of site-specific contacts to 1D nanostructures. Two novel applications, which would be difficult to achieve with conventional EBL, were demonstrated and discussed. In the first instance, three-terminal transport measurements were performed with Y-junction carbon nanotubes. The regulation of a source-drain channel current in one branch of such a nanotube by the application of a gate voltage to the third terminal was demonstrated for the first time. In the second case, electromechanical degradation of silver nanowires was investigated by in-situ biasing in a TEM. Even though contact resistance effects limited the $I-V$ measurements, the degradation of the nanowires by core melting followed by sheath conductivity was successfully observed. We believe that with continued refinement the technique of direct-write FIB based lithography can enable a wide variety of electrical transport investigations in nanotechnology research.

Acknowledgment. This work was supported by the Office of Science, Basic Energy Sciences, Division of Materials Sciences of the U.S. Department of Energy under Contract No. DE-AC03-76SF00098. We thank Prof. Apparao M. Rao of Clemson University for Y-junction nanotube synthesis. We thank Andrea Tao of the University of California, Berkeley for Ag nanowire synthesis.

References

(1) Lieber, C. M. *MRS Bull.* **2003**, *28*, 486.
(2) Molhave, K.; Madsen, D. N.; Rasmussen, A. M.; Carlsson, A.; Appel, C. C.; Brorson, M.; Jacobsen, C. J. H.; Boggild, P. *Nano Lett.* **2003**, *3*, 47.
(3) Madsen, D. N.; Molhave, K.; Mateiu, R.; Rasmussen, A. M.; Brorson, M.; Jacobsen, C. J. H.; Boggild, P. *Nano Lett.* **2003**, *3*, 1499.
(4) Melngailis, J. *J. Vac. Sci. Technol. B* **1987**, *5*, 469.
(5) Shedd, G. M.; Dubner, A. D.; Lezec, H.; Melngailis, J. *Appl. Phys. Lett.* **1986**, *49*, 1584.
(6) Silvis-Cividjian, N.; Hagen, C. W.; Kruit, P.; Stam, M. A. J.v.d.; Groen, H. B. *Appl. Phys. Lett.* **2003**, *82*, 3514.
(7) Gopal, V.; Stach, E. A.; Radmilovic, V. R.; Mowat, I. A. *Appl. Phys. Lett.* **2004**, *85*, 49.
(8) Gothard, N.; Daraio, C.; Gaillard, J.; Zidan, R.; Jin, S.; Rao, A. M. *Nano Lett.* **2004**, *4*, 213.
(9) Andriotis, A. N.; Menon, M.; Srivastava, D.; Chernozatonskii, L. *Appl. Phys. Lett.* **2001**, *79*, 266.
(10) Papadopoulos, C.; Rakitin, A.; Li, J.; Vedeneev, A. S.; Xu, J. M. *Phys. Rev. Lett.* **2000**, *85*, 3476.
(11) Tao, A.; Kim, F.; Hess, C.; Goldberger, J.; He, R.; Sun, Y.; Xia, Y.; Yang, P.; *Nano Lett.* **2003**, *3*, 1229.

NL0492133